Ectonucleotidases of the Rabbit Ciliary Body Nonpigmented Epithelium

Nasser A. Farahbakhsh

Purpose. To investigate the expression of both the message and function of ENPP1 (a member of the ectonucleotide pyrophosphatase/phosphodiesterase family, also known as PC-1), NTPD1 (a member of the ectonucleoside 5′-triphosphate diphosphohydrolase family, CD39), and ecto-5′-nucleotidase (CD73) in rabbit ciliary body nonpigmented epithelial (NPE) cells.

Methods. Reverse transcription–polymerase chain reaction (RT-PCR) analysis was used to reveal the presence of mRNAs of ectonucleotidases in NPE cells. Real-time fluorescence ratio imaging of the intact fura-2–loaded NPE cells was used to record changes in the intracellular calcium concentration.

Results. RT-PCR analysis revealed the expression of mRNAs for ENPP1, NTPD1, and ecto-5′-nucleotidase, but not NTPD2 (ecto-ATPase, or CD39L1), in the rabbit NPE cells. The ENPP1 inhibitor pyridoxal-phosphate-6-azophenyl-2′,4′-disulfonate (PPADS), and to a lesser degree the nonspecific ectonucleotidase antagonist 6-*N*,*N*-diethyl-β-γ-dibromomethylene-D-adenosine 5-triphosphate (ARL 67156), reduced the $[Ca^{2+}]_i$ increase elicited by the combination of acetylcholine (ACh) and cAMP. However, both inhibitors significantly enhanced the $[Ca^{2+}]_i$ increase generated by uridine triphosphate (UTP). The ecto-5′-nucleotidase inhibitor αβ-meADP significantly diminished the $[Ca^{2+}]_i$ increase evoked by ACh+cAMP, but not that generated by UTP. The A_1-specific adenosinergic receptor antagonist 8-cyclopentyl-1,3-dipropylxanthine (DPCPX) significantly blocked the response to ACh+cAMP.

Conclusions. These observations suggest that rabbit NPE cells possess at least three distinct ectonucleotidases capable of catalyzing the stepwise hydrolysis of adenine and pyrimidine nucleotides, as well as cAMP, thus shaping the purinergic-receptor–coupled signaling in these cells. (*Invest Ophthalmol Vis Sci.* 2003;44:3952–3960) DOI:10.1167/iovs.02-1213

The nonpigmented cell layer of the ciliary body forms the epithelium responsible for secretion of aqueous humor (AH) into the posterior chamber of the eye.[1,2] Along with AH, these cells have been shown to synthesize and release a number of regulatory agents with autocrine and paracrine characteristics.[3] In particular, the release of adenosine 3′,5′-cyclic monophosphate (cAMP) and adenosine 5′-triphosphate (ATP) in response to neural, hormonal, mechanical, and osmotic stimuli has been reported.[4–11] Furthermore, both cAMP and adenosine have been suggested to play a role in the regulation of AH inflow, as well as in its outflow.[7,10,12–16]

The topical ocular application of the adrenergic agonist, epinephrine causes an increase in both cAMP[4–6] and adenosine[14–16] in the AH withdrawn from the anterior chamber of the rabbit eye. The cellular origin of neither cAMP nor adenosine has yet been identified. Neufeld and Sears[5] reported no detectable change in the posterior chamber cAMP level in response to topical epinephrine; however, this finding was later questioned.[6] In vitro measurements show an increase in the intracellular level of cAMP in ciliary body epithelial cells in response to a variety of adenylyl cyclase activating factors (G_s-coupled receptors agonists, forskolin and cholera toxin[5,7–9]). A parallel increase in the extracellular concentration of cAMP in intact rabbit ciliary processes has been shown,[7] suggesting that nonpigmented epithelial (NPE) cells covering ciliary processes can release cAMP.

The presence of ATP in aqueous humor has been known for some time.[17] ATP is released from sensory nerve endings[18]; however, a recent report suggests that ciliary body epithelial cells may also be a source of ATP.[11] Because no adenosine transporter as yet has been shown to be present in these cells, it appears possible that adenosine present in AH is a hydrolytic product of cAMP and/or ATP.

Here, for the first time, evidence is provided of the presence in the rabbit NPE cells of both the message and function of three ectonucleotidases capable of catalyzing hydrolysis of adenine and pyrimidine nucleotides, as well as cAMP, and thus, forming adenosine (or uridine). Furthermore, it is shown that these ectonucleotidases significantly modify the purine and pyrimidine nucleotide-activated calcium signaling in NPE cells.

Materials and Methods

Tissue Isolation and Experimental Setup

For intracellular calcium ($[Ca^{2+}]_i$) measurements, intact ciliary body epithelial processes were isolated from pigmented rabbits by procedures previously described.[19] Briefly, rabbits weighing 2 to 3 kg were killed with a lethal dose of pentobarbital sodium. The eyes were rapidly enucleated, rinsed in HEPES-buffered Ringer solution (formulation described later), and hemisected. These procedures adhered to the ARVO Statement for the Use of Animals in Ophthalmic and Vision Research. Single processes were sectioned from the ciliary body by cutting along the base of the process from the iridial margin to the pars plana. Individual processes were laid on their sides in Ringer in the center of 35-mm Petri dishes that had been modified by cementing a glass coverslip over a hole drilled into the bottom of the dish. The processes were covered and held down with a 2- to 3-mm^2 piece of glass coverslip, to provide mechanical stability. A Plexiglas insert was placed in the chamber to reduce the chamber volume to 250 μL. The process was continually superfused with Ringer or a test solution at a rate of 10 $mL \cdot min^{-1}$.

For RT-PCR analysis, the NPE layer was isolated by incubating pieces of the rabbit ciliary body in low-calcium Ringer (10 mM EGTA) for up to 3 hours, at 37°C, after which NPE layer was gently separated from the rest of ciliary body with the help of two pairs of forceps. As reported previously, this method yields a greater than 99% pure NPE cell preparation.[20]

From the Department of Physiological Science, University of California, Los Angeles, California.

Supported by Grant EY06969 from the National Eye Institute.

Submitted for publication November 26, 2002; revised March 7 and May 16, 2003; accepted May 29, 2003.

Disclosure: **N.A. Farahbakhsh**, None

The publication costs of this article were defrayed in part by page charge payment. This article must therefore be marked "*advertisement*" in accordance with 18 U.S.C. §1734 solely to indicate this fact.

Corresponding author: Nasser A. Farahbakhsh, Department of Physiological Science, 4817 Life Sciences, University of California, Los Angeles, CA 90095-1606; farahbak@ucla.edu.

Investigative Ophthalmology & Visual Science, September 2003, Vol. 44, No. 9

Solutions

HEPES-buffered Ringer was of the following composition (in mM): 137 NaCl, 4.3 KCl, 1.7 $CaCl_2$, 0.8 $MgCl_2$, 10 sucrose, 7 glucose, 10 HEPES, and 6 NaOH (pH 7.6, 293–298 mOsm). Low-calcium Ringer was prepared by substituting 10 mM EGTA for equiosmolar NaCl (extracellular free calcium concentration, $[Ca^{2+}]_o$, <3 nM). Acetylcholine (ACh), adenosine (Ado), adenosine 3′,5′-cyclic monophosphate (cAMP), adenosine 5′-($\alpha\beta$ methylene) diphosphate ($\alpha\beta$-meADP), adenosine 5′-($\alpha\beta$ methylene) triphosphate ($\alpha\beta$-meATP), adenosine 5′-($\beta\gamma$ methylene) triphosphate ($\beta\gamma$-meATP), 8-cyclopentyl-1,3-dipropylxanthine (DPCPX), 6-*N*,*N*-diethyl-β-γ-dibromomethylene-D-adenosine 5-triphosphate (ARL 67156), ionomycin, pyridoxal-phosphate-6-azophenyl-2′,4′-disulfonate (PPADS), uridine 5′-triphosphate (UTP), and Ringer salts were purchased from Sigma-Aldrich (St. Louis, MO). All drugs were prepared as concentrated stocks and stored at −20°C.

Fura-2 Loading and Ca^{2+} Imaging

Ciliary processes were loaded with 10 μM fura 2-acetoxymethyl ester (fura-2/AM; Molecular Probes Inc., Eugene, OR) for 45 to 120 minutes at room temperature and then washed with Ringer. $[Ca^{2+}]_i$ measurements were made at 37°C, as described previously.[19] The method of Owen[21] was used to estimate the error in calculating $[Ca^{2+}]_i$. Only the results of experiments in which the relative error remained below 15% were used. Data are shown in figures as calibrated $[Ca^{2+}]_i$, in nanomolar, and in insets in the figures as average ± SE. For these presentations, unpaired Student's *t*-test was used for statistical analysis. $P < 0.05$ was considered significant. In the text, the data is presented as either peak $[Ca^{2+}]_i$ increase over the resting level immediately before the drug application (peak − base), in nanomolar, or as a percentile increase over the baseline (100 · (peak − base)/base). The effects of inhibitors are expressed as the relative decrease in the percentile increase in response to each agonist in the presence and absence of the blocker (100 · (1 − percentile increase in the presence/percentile increase in the absence). For this latter form of presentation, paired *t*-test was used. Again, $P < 0.05$ was considered significant.

Reverse Transcription–Polymerase Chain Reaction Analysis

For RNA isolation, the acid guanidinium-phenol-chloroform method of Chomczynski and Sacchi[22] was used. A commercially available enzyme was used for cDNA synthesis (Super Script II; Invitrogen Life Technologies, Gaithersburg, MD), according to the manufacturer's instructions. The cDNA was then used as a template for amplification in PCR. The primer sets used for ENPP1 (ectonucleotide pyrophosphatase/phosphodiesterase 1, also known as PC-1), NTPD1 (ectonucleoside 5′-triphosphate diphosphohydrolase, NTPDase, also known as ectoapyrase or CD39), NTPD2 (ectonucleoside 5′-triphosphatase, NTPase, also known as ecto-ATPase or CD39L1), and ecto-5′ (ecto-5′-nucleotidase, CD73), are listed in the following section. The primer set for each ectoenzyme was designed using the common segments of its human, mouse, and rat homologues cDNAs. For each primer set, the GenBank accession number for all homologues used are given in the first parentheses. The following pair of numbers refers to the position of each oligonucleotide fragment in the human homologue. Finally, the calculated melting temperature for each oligonucleotide is given in the second parentheses.

ENPP1 (human, NM_006208; mouse, NM_008813; rat, NM_053535): forward, 1043–1077, TCA GTA CCA TTT GAA GAA AGG ATT TTA GCT GTT CT (70.92°C); reverse, 1630–1605, GTC AGA GCC ATG AAA TCC ACT TCC AC (71.28°C).

NTPD1 (human, NM_001776; mouse, NM_009848; rat, NM_022587): forward, 541–560, CTA CCC CTT TGA CTT CCA GG (62.36°C); reverse, 1098–1080, GCA CAC TGG GAG TAA GGG C (64.64°C).

NTPD2 (human, NM_001246; mouse, NM_009849; rat, AF276940): forward, 515–532 AAG GGG TGT TTG GCT GGG (67.15°C); reverse, 1360–1340, GCA GCA GGA GRR CRA CCC AGG (R stands for G or A) (67.14°C).

Ecto-5′ (human, NM_002526; mouse, NM_011851; rat, NM_021576): forward, 388–411, GGC ACT GGG AAA TCA TGA ATT TGA (69.50°C); reverse, 1287–1269, GCA GCC AGG TTC TCC CAG G (69.47°C).

For each ectoenzyme, several different annealing temperatures around the melting temperature were tried for the PCR reaction. Cycling conditions were 1 minute at 95°C, 1 minute at the annealing temperature, and 1 minute at 72°C. This cycle was repeated 35 times. Ten microliters of each PCR product was then electrophoresed on 1.5% agarose gel containing ethidium bromide.

Results

We have previously reported that in NPE cells of the rabbit ciliary body, stimulation of the A_1 adenosinergic receptors, though producing a very small increase in the $[Ca^{2+}]_i$ on its own, can synergistically enhance the $[Ca^{2+}]_i$ increase induced by the muscarinic receptor activation.[23] Figure 1A shows that adenosine has a similar effect on the $[Ca^{2+}]_i$ increase evoked by the $P2Y_2$-receptor agonist uridine 5′-triphosphate (UTP). At 1 μM, adenosine enhanced the effect of 100 μM UTP on the $[Ca^{2+}]_i$ by a factor of 3.0 ± 1.2 (mean ± SE, $n = 3$). The low concentration of adenosine needed to generate such synergistic effects (1 μM in Figs. 1A, 1C, 2 μM in Fig. 1B) has allowed us to use the changes in $[Ca^{2+}]_i$ as a sensitive functional assay for adenosine generation by the NPE cells' surface-bound ectoenzymes.

NPE Cell Ectophosphodiesterase/Nucleotide Pyrophosphatase Activity

As was the case for adenosine (Fig. 1A), cAMP (Fig. 1B), $\alpha\beta$-meATP (Fig. 1C), or $\beta\gamma$-meATP (Fig. 1D) did not significantly increase the $[Ca^{2+}]_i$ when applied alone (all at 100 μM concentration), in agreement with our recent report.[24] However, cAMP (Fig. 1B) and $\beta\gamma$-meATP (Fig. 1D), but not $\alpha\beta$-meATP (Fig. 1C), significantly enhanced the ACh-induced $[Ca^{2+}]_i$ increase. cAMP, at 100 μM, increased the response to 20 μM ACh 3.7 ± 0.5 times ($n = 4$), whereas $\beta\gamma$-meATP at 100 μM enhanced the ACh-induced response by a factor of 10.0 ± 2.8 ($n = 3$). In the presence of 100 μM $\alpha\beta$-meATP, ACh evoked a $[Ca^{2+}]_i$ increase that was 66% ± 5% of the control ($n = 4$). Compared with adenosine (Figs. 1B, 1C), cAMP (Fig. 1B) and $\beta\gamma$-meATP (Fig. 1D) appear to be approximately 50 and 100 times, respectively, less effective in enhancing the response to ACh.

The effect of cAMP on the ACh-induced response was not mimicked by the membrane-permeable cAMP analogues 8-bromo-cAMP or dibutyryl-cAMP, ruling out a role for the intracellular cAMP (data not shown). Furthermore, in the absence of a $[Ca^{2+}]_i$ increase in response to either $\alpha\beta$-meATP or $\beta\gamma$-meATP, a role for P2 purinergic receptors coupled to calcium signaling can be ruled out (see Ralevic and Burnstock[25]). Thus, it appears that the effects of both cAMP and $\beta\gamma$-meATP on the muscarinic receptor–coupled signaling in the rabbit NPE cells, may be mediated by adenosine formed as a result of the degradation of these agents by the extracellular hydrolytic enzymes. The formation of adenosine from cAMP or $\beta\gamma$-meATP requires a two-step hydrolytic activity. In the first step cAMP or $\beta\gamma$-meATP is converted to 5′-AMP. The breakdown of the extracellular cAMP requires the expression of an ectophosphodiesterase.[26–28] Similarly, because $\beta\gamma$-meATP is not a substrate for either the ATPase or ATP-diphosphohydrolase,[29,30] hydrolysis of $\beta\gamma$-meATP is dependent on the presence of an

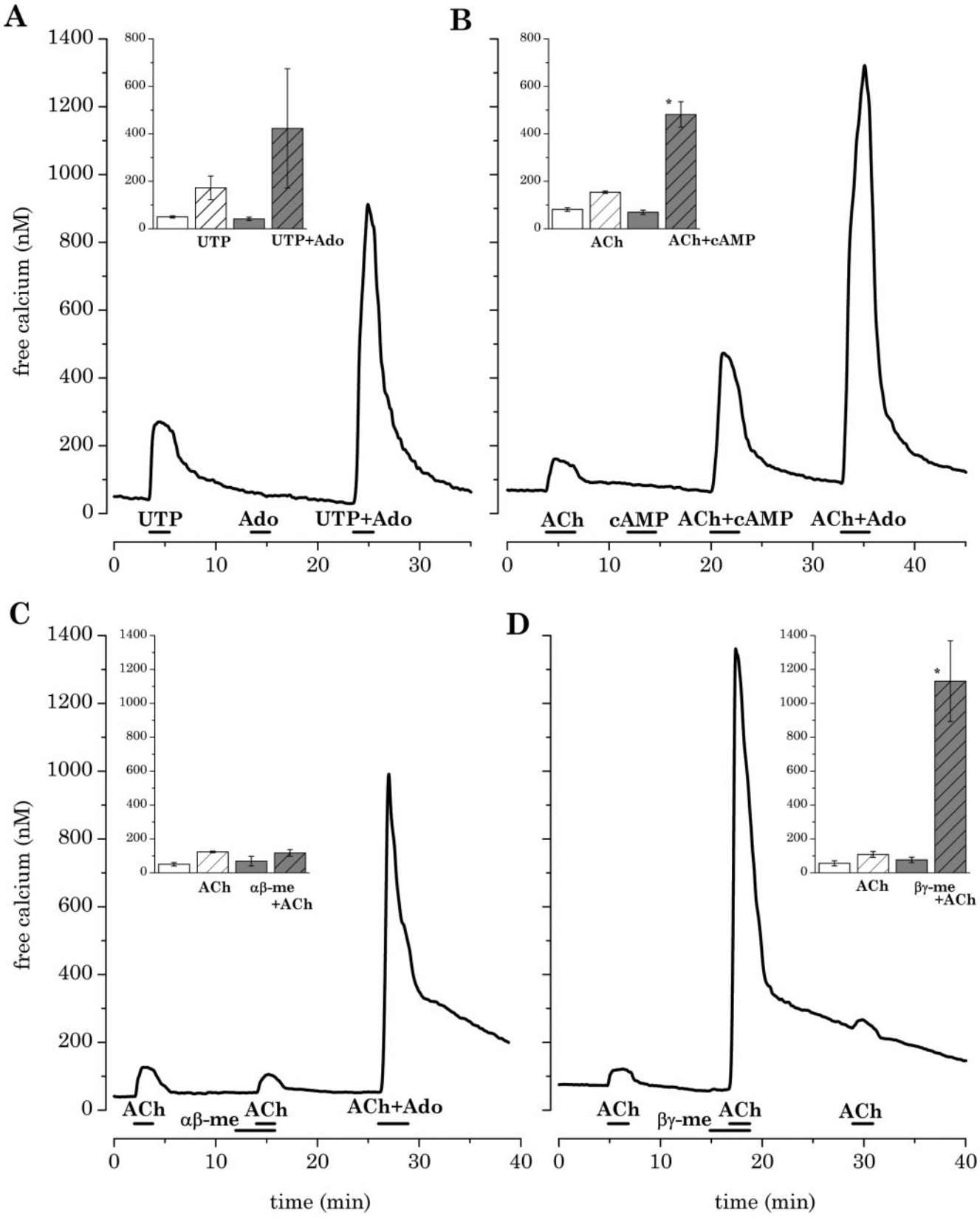

FIGURE 1. Adenosine, cAMP, and $\beta\gamma$-meATP, but not $\alpha\beta$-meATP, synergistically enhanced the increase in the intracellular free calcium concentration ($[Ca^{2+}]_i$) generated by ACh or UTP in the rabbit ciliary body NPE cells. (**A**) The change in the $[Ca^{2+}]_i$ recorded in intact NPE cells loaded with fura-2, is shown as a function of time. The responses to 100 μM UTP, 1 μM adenosine, and 100 μM UTP+1 μM adenosine, recorded from the same tissue, are shown. *Horizontal lines*: the durations of exposure to UTP, adenosine (Ado), and UTP+adenosine (UTP+Ado). *Inset*: average ± SE $[Ca^{2+}]_i$ measured before the application of UTP or UTP+Ado and at the peak of response to UTP or UTP+Ado in three similar experiments. (**B**) The changes in the NPE cell $[Ca^{2+}]_i$ in response to the sequential application of 20 μM acetylcholine (ACh), 100 μM cAMP

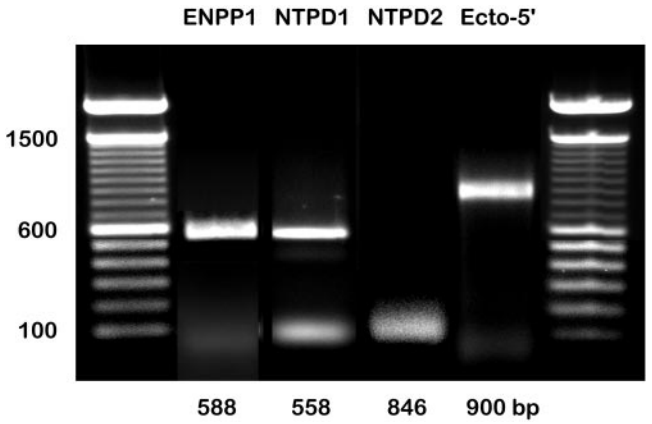

FIGURE 2. RT-PCR analysis of mRNAs for ectonucleotidases ENPP1, NTPD1, NTPD2, and 5′-nucleotidase in the rabbit NPE cells. Shown is the outcome of agarose gel electrophoresis of the PCR products. *Left* and *right lanes*: size marker (100-bp standard). *Middle four columns*: for each ectonucleotidase the expected cDNA segment length is shown at the *bottom*. The annealing temperatures for ENPP1, NTPD1, NTPD2, and 5′-nucleotidase were 68.7°C, 58.5°C, 58.8°C, and 63.9°C, respectively.

ectopyrophosphatase.[31–33] In the second step, 5′-AMP is hydrolyzed to adenosine by either a 5′-nucleotidase,[34] or an alkaline phosphatase.[35]

Expression of Ectonucleotidase mRNA in the Rabbit NPE Cells

Because no rabbit homologue of any ectonucleotidase has been characterized, a homology-based PCR approach was used to investigate the expression of several ectonucleotidase mRNAs in the NPE cells. Based on this strategy, specific primer pairs corresponding to common cDNA segments of human, mouse, and rat homologues of each ectonucleotidase were designed and tested (see the Methods section). Figure 2 shows the results of the RT-PCR performed on the cDNA prepared from the rabbit NPE cells, confirming expression of the mRNA for ENPP1, NTPD1, and ecto-5′-nucleotidase. The expression of mRNA for NTPD2 (ecto-ATPase, or CD39L1) could not be confirmed. The functional expression of ENPP1 and the 5′-nucleotidase on the NPE cell membrane would suffice to explain the results shown in Figures 1B and 1D (see Zimmermann[36]). ENPP1 is capable of hydrolyzing both cAMP,[26–28] and $\beta\gamma$-meATP,[31–33] to 5′-AMP, which is then metabolized by the ecto-5′-nucleotidase to form adenosine.[34] The failure of $\alpha\beta$-meATP to enhance the ACh-induced $[Ca^{2+}]_i$ increase (Fig. 1C), can also be explained by the fact that, because of the relative position of methylene in its phosphate chain, it is not metabolized by either ENPP1 or NTPD1.[30,31]

Role of the NPE Cell Ectonucleotidases in Generation of the Synergistic Response to cAMP and Acetylcholine

To demonstrate the sequential steps involved in the hydrolysis of cAMP and the activation of the A_1 receptor the effects of PPADS, ARL 67156, $\alpha\beta$-meADP, and DPCPX, on the synergistic response to the combination of cAMP and ACh, were examined. PPADS inhibits the ectonucleotide pyrophosphatase/phosphodiesterase in the rat C6 glioma cells with an IC_{50} of 12 ± 3 μM,[37] whereas having a much lower affinity for the NTPD1 in the rat vas deferens,[38] *Xenopus* oocytes,[39] and the rat ATP-diphosphohydrolase heterologously expressed in CHO cells.[40] In the rabbit NPE cells, PPADS at 25 μM, significantly reduced the response to the combination of ACh and cAMP (Fig. 3A). In three similar experiments, the response to ACh and cAMP in the presence of PPADS was 13% ± 2% of the control ($P < 0.021$). The effect of PPADS was partially reversible (Fig. 3A). After a 10-minute washing period, the response was 58% ± 15% of the control ($n = 3$, $P < 0.005$, compared with the response in the presence of PPADS).

ARL 67156, a structural analogue of ATP, is considered a nonspecific ectotriphosphate nucleotidase inhibitor.[36] It has been reported to inhibit the ATP diphosphohydrolase (ATPDase) activity in rat vas deferens, with an IC_{50} of 7.9 μM,[38] and in human blood with an IC_{50} of 25 μM.[41] Its effects on members of the ENPP family have not been reported. In the rabbit NPE cells, ARL 67156 at 50 μM inhibited the synergistic response to ACh and cAMP by 70% ± 12% ($n = 4$, $P < 0.046$, Fig. 3B). After a 10-minute washing, the recovery was not significant (31% ± 12% of the control, $n = 4$, $P > 0.466$).

The 5′-nucleotidase inhibitor $\alpha\beta$-meADP,[34] also induced a significant inhibition of the response to ACh and cAMP (Fig. 3C). In the presence of 100 μM $\alpha\beta$-meADP, the response to ACh and cAMP was 9% ± 5% of the control ($n = 3$, $P < 0.046$). A 10- minute washing led to a partial recovery (23% ± 12% of the control, $n = 3$, $P > 0.151$).

The A_1-adenosinergic receptor antagonist DPCPX[23,42] also significantly reduced the size of the $[Ca^{2+}]_i$ increase generated by the ACh and cAMP combination (Fig. 3D). In the presence of 100 nM DPCPX, the response to ACh and cAMP was only 10% ± 2% of the control ($n = 5$, $P < 0.013$). After a 10-minute wash, the response recovered to 20% ± 3% of the control ($n = 5$, $P > 0.06$). The results shown in Figure 3 suggest that synergistic effect of cAMP on the ACh-induced $[Ca^{2+}]_i$ increase requires, at minimum, the hydrolytic activities of both a PPADS- and ARL 67156-sensitive phosphodiesterase, and an $\alpha\beta$-meADP-sensitive 5′-nucleotidase, to form the agonist required for the activation of a DPCPX-inhibitable P1 receptor.

Effect of NPE Cell Ectonucleotidases on the UTP-Induced $[Ca^{2+}]_i$ Increase

We have recently reported that rabbit NPE cells express the metabotropic $P2Y_2$ receptor linked to the calcium signaling in these cells. However, the dose–response curve for the $P2Y_2$-receptor agonist UTP is rather steep (the Hill coefficient, n_H =

(cAMP), 20 μM ACh+100 μM cAMP (bar ACh+cAMP), and 20 μM ACh+2 μM adenosine (ACh+Ado). *Inset*: average ± SE $[Ca^{2+}]_i$ measured before the application of ACh or ACh+cAMP and at the peak of response to ACh or ACh+cAMP in four similar experiments. *Statistically significant difference compared with the response to ACh alone ($P < 0.005$). (**C**) Responses of NPE cell $[Ca^{2+}]_i$ to 20 μM ACh (ACh), 100 μM $\alpha\beta$-meATP ($\alpha\beta$-me), and 20 μM ACh+1 μM adenosine (ACh+Ado). The overlap of the *horizontal lines* represents the period in which both $\alpha\beta$-meATP and ACh were applied. *Inset*: average ± SE $[Ca^{2+}]_i$ measured in the absence and presence of $\alpha\beta$-meATP, before the application of ACh, or at the peak of response to ACh in four similar experiments. (**D**) Changes in NPE cell $[Ca^{2+}]_i$ generated by 20 μM ACh (ACh) and 100 μM $\beta\gamma$-meATP ($\beta\gamma$-me). *Inset*: average ± SE $[Ca^{2+}]_i$ measured in the absence and presence of $\beta\gamma$-meATP, before the application of ACh, or at the peak of response to ACh in three similar experiments. *$P < 0.01$. In all inset bar graphs, *solid bars* represent the baseline $[Ca^{2+}]_i$ level before application of the agent listed, and *hatched bars* show the peak $[Ca^{2+}]_i$ increase in the presence of that agent.

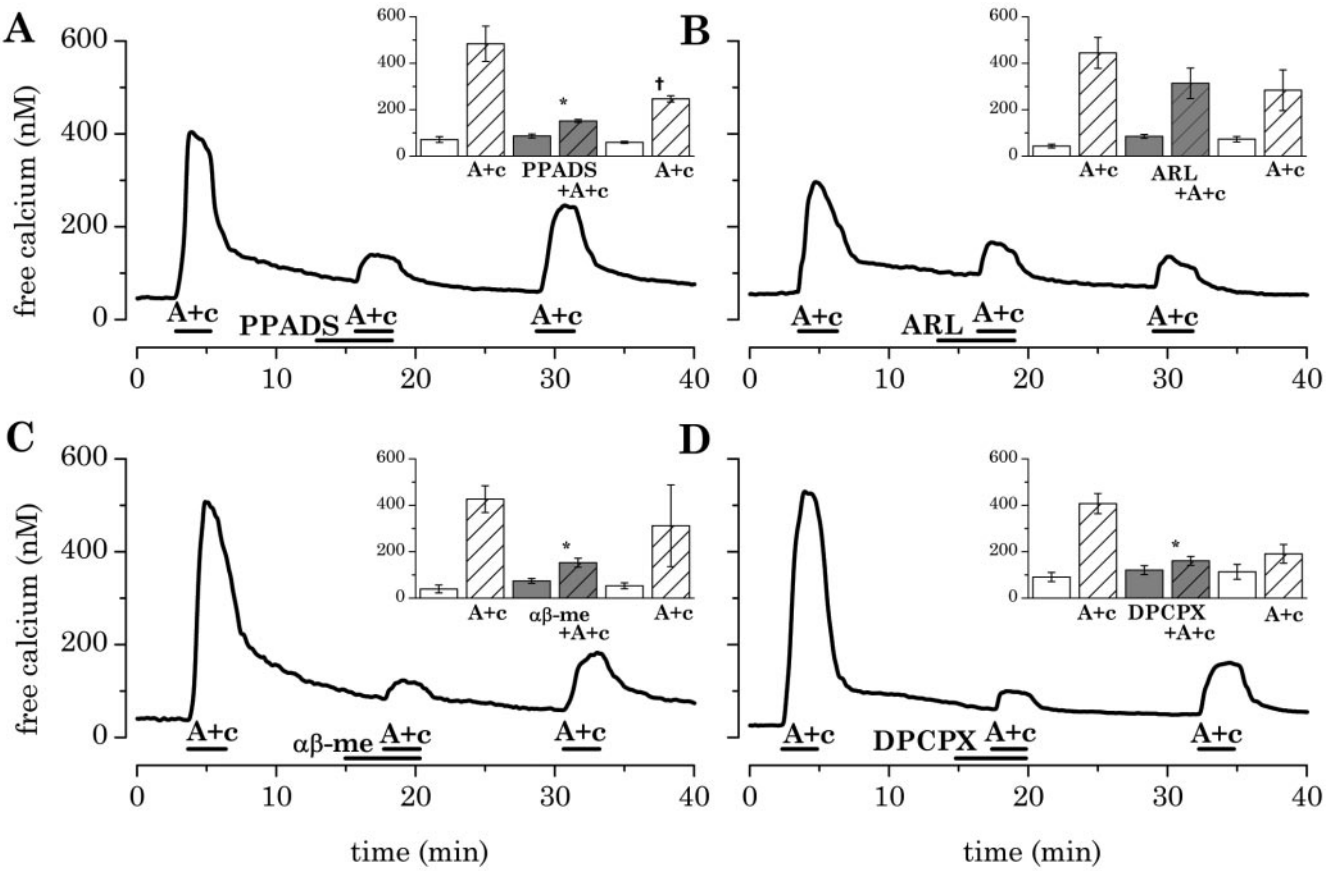

FIGURE 3. The synergistic response to ACh and cAMP was inhibited by pretreatment with PPADS, ARL 67156, $\alpha\beta$-meADP, or DPCPX. (**A**) The $[Ca^{2+}]_i$ increases in NPE cells in response to 20 μM ACh+100 μM cAMP (A+c), before, during, and after exposure to 25 μM PPADS. *Inset*: average ± SE $[Ca^{2+}]_i$ measured in the absence and presence of PPADS, before the application of ACh+cAMP, or at the peak of response to ACh+cAMP in three similar experiments. *Statistically significant difference †$P < 0.025$, with the control response. $P < 0.004$, recovery compared with the response in the presence of PPADS. (**B**) The inhibitory effect of 50 μM ARL 67156 (ARL) on the $[Ca^{2+}]_i$ increase induced by the combination of 20 μM ACh+100 μM cAMP. *Inset*: average ± SE $[Ca^{2+}]_i$ measured in the absence and presence of ARL 67156, before the application of ACh+cAMP or at the peak of response to ACh+cAMP in four similar experiments. (**C**) The $[Ca^{2+}]_i$ increases evoked by 20 μM ACh+100 μM cAMP in the absence and presence of 100 μM $\alpha\beta$-meADP ($\alpha\beta$-me). *Inset*: average ± SE $[Ca^{2+}]_i$ measured in the absence and presence of $\alpha\beta$-meADP, before the application of ACh+cAMP or at the peak of response to ACh+cAMP in three similar experiments. *$P < 0.024$. (**D**). The ACh+cAMP-evoked response was also significantly inhibited by 100 nM DPCPX. *Inset*: average ± SE $[Ca^{2+}]_i$ measured in the absence and presence of DPCPX, before the application of ACh+cAMP or at the peak of response to ACh+cAMP in five similar experiments. *$P < 0.002$. In all inset bar graphs, *solid bars* represent the baseline $[Ca^{2+}]_i$ level before application of the agent listed, and *hatched bars* show the peak $[Ca^{2+}]_i$ increase in the presence of that agent.

13.0 ± 2.8), and has an EC_{50} of 42.8 ± 1.1 μM.[24] These characteristics are quite different from those reported for the cloned $P2Y_2$ receptor[43] and suggest significant hydrolysis of UTP by ectonucleotidases.[44] UTP is a substrate for both the rat ecto-ATP diphosphohydrolase heterologously expressed in CHO cells[40] and the ectonucleotide pyrophosphatase in rat C6 glioma cells.[31]

Figures 4A and 4B show that inhibition of the ectonucleotidases in the rabbit NPE cells by either PPADS (Fig. 4A), or ARL 67156 (Fig. 4B) can significantly enhance the response to 100 μM UTP. PPADS, at 25 μM, enlarged the response to UTP by a factor of 3.7 ± 0.7 ($n = 4$, $P < 0.034$), whereas 50 μM ARL 67156 increased the response 3.3 ± 0.6 times ($n = 3$, $P < 0.006$). Both values are near the theoretical factor of 3.

Neither $\alpha\beta$-meADP (Fig. 4C), nor DPCPX (Fig. 4D), had a significant effect on the UTP-induced $[Ca^{2+}]_i$ increase. In the presence of 100 μM $\alpha\beta$-meADP, the response to 100 μM UTP was 80% ± 6% of the control (corrected for the receptor desensitization, $n = 3$, $P > 0.065$). Similarly, in the presence of 100 nM DPCPX, the response to UTP was 77% ± 13% of the control (corrected, $n = 4$, $P > 0.072$). To rule out a role for the A_1 receptor in the enhancement of the response to UTP by PPADS, the effect of the combined application of 25 μM PPADS and 100 nM DPCPX on the UTP-induced $[Ca^{2+}]_i$ increase was also determined. In four experiments, the combination of PPADS and DPCPX enhanced the response to UTP 2.4 ± 0.2 times ($P < 0.002$, data not shown).

DISCUSSION

This is the first report of studies revealing the presence of a cascade of ectonucleotidase activities in the rabbit ciliary body NPE cells, capable of stepwise hydrolytic metabolizing of purine and pyrimidine nucleotides and cyclic nucleoside monophosphates. I have combined functional assays—the $[Ca^{2+}]_i$ measurement—with RT-PCR to show the expression of both the message and function of PC-1 (a member of the ectonucleotide pyrophosphatase/phosphodiesterase family), CD39 (a member of ectonucleoside 5′-triphosphate diphosphohydrolase family), and CD73 (ecto-5′-nucleotidase).

The functional assay used herein is based on the previously reported observation that, in NPE cells, the activation of a

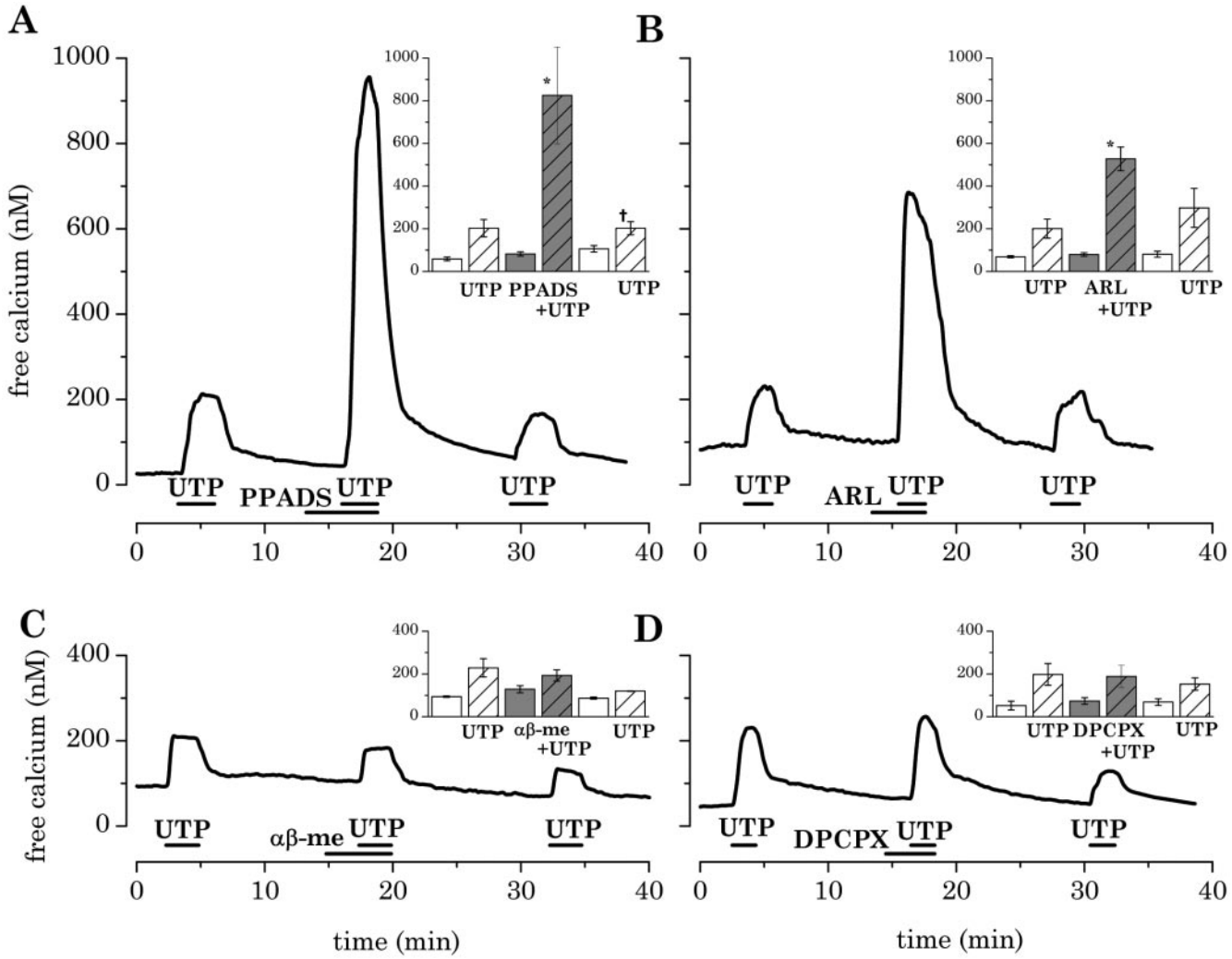

FIGURE 4. The enhancing effects of pretreatment of the NPE cells with PPADS or ARL 67156 on the UTP-induced $[Ca^{2+}]_i$ increase. (**A**) The response to 100 μM UTP, before, during, and after exposure to 25 μM PPADS. *Inset*: average ± SE $[Ca^{2+}]_i$ measured in the absence and presence of PPADS, before the application of UTP or at the peak of response to UTP in four similar experiments. *Statistically significant difference (†$P <$ 0.037) from the control response. $P < 0.037$, recovery compared to the response in the presence of PPADS. (**B**) The UTP-evoked response was also enhanced by ARL 67156 (ARL). *Inset*: average ± SE $[Ca^{2+}]_i$ measured in the absence and presence of ARL 67156, before the application of UTP or at the peak of response to UTP in three similar experiments. *$P < 0.006$. (**C**) $\alpha\beta$-meADP ($\alpha\beta$-me) at 100 μM had no significant effect on the $[Ca^{2+}]_i$ elevation generated by 100 μM UTP. *Inset*: average ± SE $[Ca^{2+}]_i$ measured in the absence and presence of $\alpha\beta$-meADP, before the application of UTP or at the peak of response to UTP in three similar experiments. (**D**) DPCPX at 100 nM concentration was also without a significant effect on the response 100 μM UTP. *Inset*: average ± SE $[Ca^{2+}]_i$ measured in the absence and presence of DPCPX, before the application of UTP or at the peak of response to UTP in four similar experiments. In all inset bar graphs, *solid bars* represent the baseline $[Ca^{2+}]_i$ level before application of the agent listed, and *hatched bars* show the peak $[Ca^{2+}]_i$ increase in the presence of that agent.

G_i-coupled receptor, such as the A_1 adenosinergic receptor, can synergistically enhance the $[Ca^{2+}]_i$ increase generated as a result of the stimulation of a G_q-linked receptor, such as the muscarinic receptor.[23] Furthermore, we have also reported that an interaction between signal transduction pathways coupled to these two receptor types, at a level preceding the formation of IP_3, may be partly responsible for generation of these synergistic responses.[45] My recent observations suggest that rabbit NPE cells express mRNAs for the $P2Y_1$, $P2Y_2$, $P2Y_6$, and $P2Y_{12}$ purinergic receptor subtypes.[46] Herein, I report that simultaneous activation of the A_1 receptor and a metabotropic P2Y receptor, such as the $P2Y_2$ (Fig. 1A) or the $P2Y_1$ receptor (not shown), can produce a similar synergistic response. The high sensitivity of this synergistic interaction for adenosine (EC_{50} = 250 nM[23]), along with the presence of both IP_3/Ca^{2+}-linked $P2Y_1$ and $P2Y_2$ receptors,[24,46] and the ectonucleotidase activity in these cells (this work), is expected therefore to allow an adenine 5′-nucleotide, such as ATP or ADP, to activate at least one P2Y receptor, whereas its metabolic product adenosine is activating the A_1 receptor. As a result, these characteristics of NPE cells have made it possible to use the synergistic $[Ca^{2+}]_i$ increase as a sensitive measure of adenosine formation by adenine nucleotides or cAMP, and thus the ectonucleotidase activity.

ENPP1

Originally discovered as the murine plasma cell differentiation antigen (PC-1), ENPP1 is a membrane glycoprotein expressed in a number of mammalian epithelial tissues, such as the ducts of salivary glands and the distal convoluted tubules of kidney, as well as in the epididymis and chondrocytes[47] and in cell lines derived from brain glial cells.[32–33] It has been known for some time that this protein is an ectoenzyme with both 5′-

nucleotide phosphodiesterase and nucleotide pyrophosphatase activity.[48,49] Its sensitivity to blockage by several P2 purinergic receptors antagonists, such as PPADS (IC_{50} = 12 ± 3 μM), has recently been reported.[37]

The evidence for the presence of ENPP1 in the rabbit NPE cells is several-fold. First, the mRNA for this protein is expressed in these cells (Fig. 2). The primer pair designed for the rabbit ENPP1 is based on two DNA segments common in the human, mouse and rat homologues of this protein. However, neither of these two primers is shared by the human, mouse or rat homologues of either ENPP2 (PD-Iα, or its splice variant autotaxin), or ENPP3 (PD-Iβ, B10, or gp130^{RB13-6}).[50–54] Thus, it is unlikely that the primer set used would recognize other ENPPs. It should be noted however, that the presence of ENPP2 in the rat ciliary body epithelium has been reported.[52] I have not determined whether other ENPPs are expressed in the rabbit NPE cells. Because the pharmacology of neither ENPP2 nor ENPP3 is known, participation of these ENPPs in the rabbit NPE cell ectonucleotidase activity cannot be ruled out.

Second, PPADS at 25 μM inhibited the $[Ca^{2+}]_i$ increase induced by cAMP+ACh by 87% (Fig. 3A). PPADS is neither an A_1 receptor antagonist[55] nor a 5′-nucleotidase inhibitor.[33] Thus, the effect of PPADS on the response to cAMP+ACh can only be attributed to its inhibitory effect on the cAMP phosphodiesterase activity and, therefore, on adenosine formation. Similarly, the ectonucleotidase inhibitor ARL 67156 at 50 μM inhibited the cAMP+ACh–induced response by 70% (Fig. 3B). ARL 67156 is reported to inhibit NTPD1 and NTPD2 activities in several tissues.[41,56–59] However, neither its effect on the 5′-nucleotidase activity nor on the A_1 receptor has been reported. Nevertheless, the similarity of the effects of ARL 67156 and PPADS on agonists tested in this study (Figs. 3, 4), suggests that ARL 67156 is also an ENPP1 inhibitor.

Third, the $[Ca^{2+}]_i$ increase generated by UTP (Fig. 4A) is very sensitive to a low concentration (25 μM) of PPADS. Contrary to its relatively higher affinity for ENPP1 in C6 glioma cells,[37] PPADS appears to be a much less effective inhibitor of the ATPase and ATPDase activity in number of tissues so far tested.[36,38–40]

Because PPADS does not increase the $[Ca^{2+}]_i$ on its own (Figs. 3A, 4A), it cannot be considered a P2Y agonist in NPE cells. Similarly, PPADS is not an agonist of the A_1 receptor (Fig. 3A). Thus, the effect of PPADS on the UTP-evoked $[Ca^{2+}]_i$ increase (Fig. 4A) can only be attributed to its inhibition of the ectonucleotidase activity, primarily that of ENPP1,[37] and therefore an increase in the UTP concentration in the vicinity of the $P2Y_2$ receptor.

Similar results were obtained with ARL 67156. Even though ARL 67156 is a weak agonist for the $P2Y_2$ receptor in the rabbit tracheal epithelium,[41] it showed no stimulatory effect on the $[Ca^{2+}]_i$ level in NPE cells (Figs 3B, 4B). Thus, the effect of ARL 67156 on the responses to UTP (Fig. 4B) appears to be solely the result of the ectonucleotidase inhibition. However, despite the fact that ARL 67156 was used at a concentration twice its reported IC_{50} for inhibition of NTPD1 and NTPD2,[41,60,61] which was also enough to block the ENPP1 activity by 70% (Fig. 3B), it appeared to be less effective than PPADS, which was also used at twice its IC_{50} for inhibition of ENPP1,[37] in enhancing the response to UTP (Fig. 4).

NTPD1

The RT-PCR analysis performed on rabbit NPE cells revealed the presence of mRNA for NTPD1 but not NTPD2 in this tissue (Fig. 2). Because the cDNAs for the rabbit homologue of these proteins have not been sequenced, my analysis relied on the homology-based primers using human, mouse, and rat homologues (see the Methods section). Thus, it is conceivable that primers designed for NTPD2 may have been inappropriate for the rabbit homologue of this enzyme. The expression of the NTPD1 mRNA, however, suggests the possibility that part of the ectonucleotidase activity in these cells may be mediated by NTPD1.

As described, ARL 67156 inhibited ENPP1 activity, in addition to its reported inhibitory effects on the ecto-ATPase and ecto-ATP diphosphohydrolase.[41,56–59] Thus, ARL 67156 should be considered as a nonspecific ectonucleotidase inhibitor. In the absence of specific inhibitors for NTPD1, direct evidence for the role this enzyme in the NPE cells purinergic signaling could not be obtained.

5′-Nucleotidase

Ecto-5′-nucleotidase catalyzes the hydrolysis of 5′-AMP to adenosine and P_i (see Zimmermann[34]). The evidence for the presence of 5′-nucleotidase in the rabbit NPE cells is, first, the RT-PCR analysis revealed the expression of mRNA for CD73 in these cells. The primers designed on the basis of common segments in cDNAs of human, mouse, and rat homologues of this enzyme polymerized a sequence with the predicted base pair length (Fig. 2).

Second, it has been known for quite some time that ADP and ATP analogues inhibit the 5′-nucleotidase activity. Among these analogues, $\alpha\beta$-meADP has the highest affinity for this enzyme.[62] The specificity of $\alpha\beta$-meADP for 5-nucleotidase is underscored by the fact that it did not inhibit NTPD1,[30] ENPP1,[32] or the A_1 receptor (data not shown). In the rabbit NPE cells, 100 μM $\alpha\beta$-meADP inhibited the cAMP-induced enhancement of the $[Ca^{2+}]_i$ increase generated by ACh by 91% (Fig. 3C). However, it did not significantly change the responses to UTP (Fig. 4C). These results suggest that almost all adenosine formed as a result of the cAMP hydrolysis is the result of the 5′-nucleotidase activity. These experiments, however, did not reveal the extent of the UMP and uridine formation from the UTP breakdown.

Modification of the NPE Cells Calcium Signaling by Ectonucleotidases

The $[Ca^{2+}]_i$ increase evoked by cAMP+ACh in the presence of 25 μM PPADS (Fig. 3A), 100 μM $\alpha\beta$-meADP (Fig. 3C), or 100 nM DPCPX (Fig. 3D) were not significantly different ($P > 0.26$, for each pair-wise comparison). In the absence of a known receptor for the extracellular cAMP,[63] these results suggest that (1) the synergistic effect of cAMP on the ACh-evoked $[Ca^{2+}]_i$ elevation is mediated by the A_1 receptor and (2) NPE cells possess an enzymatic cascade composed of ENPP1 and 5′-nucleotidase capable of sequential hydrolysis of cAMP to AMP and AMP to adenosine.

ENPP1 hydrolyzes UTP at a rate twice that of the ATP hydrolysis.[31] The metabolic product, uridine monophosphate (UMP) is a substrate for 5′-nucleotidase.[64] Thus, the same cascade of ectoenzymes can be responsible for the metabolizing of both cAMP and UTP. However, neither UMP nor uridine produced by this cascade appears to act as an agonist in the NPE cells. In particular, neither is able to stimulate the A_1 receptor. Otherwise, simultaneous activation of the A_1 receptor by UMP/uridine, and that of the $P2Y_2$ receptor by UTP, would have generated a synergistic response, such as the one shown in Figure 1A. In the absence of the A_1-receptor activation, the effect of UTP hydrolysis by ENPP1 is the reduction of its concentration in the vicinity of the $P2Y_2$ receptor and thus a decrease in both the apparent affinity and efficacy of this agonist.[24,44]

UTP is also a substrate for NTPD1.[40] The hydrolysis of UTP by NTPD1 generates both uridine diphosphate (UDP) and

UMP, the former being an agonist for the $P2Y_4$ and $P2Y_6$ receptor subtypes.[65] We have reported that UDP elicits a small $[Ca^{2+}]_i$ increase in the rabbit NPE cells,[24] and mRNA for the $P2Y_6$, but not for the $P2Y_4$, receptor subtype is expressed in these cells.[46] Thus, the hydrolytic activity of NTPD1 may also contribute to the UTP-induced calcium signaling through the $P2Y_6$-linked pathway.

Conclusion

The data presented suggest that, in addition to purinergic receptors linked to calcium signaling,[24,46] rabbit NPE cells possess ectonucleotidases capable of modifying adenine and pyrimidine nucleotide-induced responses in variety of ways, including generation of synergistic $[Ca^{2+}]_i$ increases.

It is noteworthy, however, that for these experiments the ciliary body NPE cells were mounted in a 250-μL recording chamber and superfused at a flow rate of 10 $mL \cdot min^{-1}$. Thus one chamber volume was exchanged every 1.5 seconds. Under these conditions, in the vicinity of the A_1 receptor, approximately 1% of the adenine nucleotides was converted to adenosine. In rabbit, the volume of the posterior chamber of the eye is approximately 60 μL, and the rate of aqueous humor secretion is 4 $\mu L \cdot min^{-1}$.[66] Thus, 15 minutes is needed to exchange one chamber volume. It is expected therefore that a much larger portion, and possibly all, of the adenine and pyrimidine nucleotides and cyclic nucleoside monophosphates released into the posterior chamber is hydrolyzed in vivo, leaving very little in the unhydrolyzed form to be detected.[5]

Acknowledgments

The author thanks James Tidball and Melissa Spencer for teaching RT-PCR, Michael Woodruff for valuable comments on the manuscript, and Luanna Yang and Nicholas Rogers for helping with the tissue dissections.

References

1. Brubaker RF. Flow of aqueous humor in humans. The Friedenwald Lecture. *Invest Ophthalmol Vis Sci*. 1991;32:3145–3166.
2. Krupin T, Civan MM. Physiologic basis of aqueous humor formation. In: Ritch R, Shield MB, Krupin T, eds. *The Glaucomas.* St. Louis: Mosby; 1996:251–280.
3. Coca-Prados M, Escribano J, Ortego J. Differential gene expression in the human ciliary epithelium. *Prog Retinal Eye Res*. 1999;18: 403–429.
4. Neufeld AH, Jampol LM, Sears ML. Cyclic-AMP in the aqueous humor: the effects of adrenergic agents. *Exp Eye Res*. 1972;14: 242–250.
5. Neufeld AH, Sears ML. Cyclic-AMP in ocular tissues of the rabbit, monkey, and human. *Invest Ophthalmol*. 1974;13:475–477.
6. Rowland JM, Potter DE. Effects of adrenergic drugs on aqueous cAMP and cGMP and intraocular pressure. *Albrecht Von Graefes Arch Klin Exp Ophthalmol*. 1979;212:65–75.
7. Gregory D, Sears M, Bausher L, Mishima H, Mead A. Intraocular pressure and aqueous flow are decreased by cholera toxin. *Invest Ophthalmol Vis Sci*. 1981;20:371–381.
8. Bartels SP, Roth HO, Neufeld AH. Effects of intravitreal cholera toxin on adenosine 3′,5′-monophosphate, intraocular pressure, and outflow facility in rabbits. *Invest Ophthalmol Vis Sci*. 1981; 20:410–414.
9. Bartels SP, Lee SR, Neufeld AH. Forskolin stimulates cyclic AMP synthesis, lowers intraocular pressure and increases outflow facility in rabbits. *Curr Eye Res*. 1982;2:673–681.
10. Caprioli J, Sears M, Bausher L, Gregory D, Mead A. Forskolin lowers intraocular pressure by reducing aqueous inflow. *Invest Ophthalmol Vis Sci*. 1984;25:268–277.
11. Mitchell CH, Carre DA, McGlinn AM, Stone RA, Civan MM. A release mechanism for stored ATP in ocular ciliary epithelial cells. *Proc Natl Acad Sci USA*. 1998;95:7174–7178.
12. Caprioli J, Sears M. Combined effect of forskolin and acetazolamide on intraocular pressure and aqueous flow in rabbit eyes. *Exp Eye Res*. 1984;39:47–50.
13. Sears ML, Neufeld AH. Adrenergic modulation of the outflow of aqueous humor (editorial). *Invest Ophthalmol*. 1975;14:83–86.
14. Crosson CE. Adenosine receptor activation modulates intraocular pressure in rabbits. *J Pharmacol Exp Ther*. 1995;273:320–326.
15. Crosson CE, Petrovich M. Contributions of adenosine receptor activation to the ocular actions of epinephrine. *Invest Ophthalmol Vis Sci*. 1999;40:2054–2061.
16. Crosson CE. Intraocular pressure responses to the adenosine agonist cyclohexyladenosine: evidence for a dual mechanism of action. *Invest Ophthalmol Vis Sci*. 2001;42:1837–1840.
17. Greiner JV, Chanes LA, Glonek T. Comparison of phosphate metabolites of the ocular humors. *Ophthalmic Res*. 1991;23:92–97.
18. Maul E, Sears M. ATP is released into the rabbit eye by antidromic stimulation of the trigeminal nerve. *Invest Ophthalmol Vis Sci*. 1979;18:256–262.
19. Farahbakhsh NA, Cilluffo MC. Synergistic effect of adrenergic and muscarinic receptor activation on $[Ca^{2+}]_i$ in rabbit ciliary body epithelium. *J Physiol*. 1994;477:215–221.
20. Fain GL, Cilluffo MC, Fain MJ, Lee DA. Isolation of non-pigmented epithelial cells from rabbit ciliary body. *Invest Ophthalmol Vis Sci*. 1988;29:817–821.
21. Owen CS. Spectra of intracellular Fura-2. *Cell Calcium*. 1991;12: 385–393.
22. Chomczynski P, Sacchi N. Single-step method of RNA isolation by acid guanidinium thiocyanate- phenol-chloroform extraction. *Anal Biochem*. 1987;162:156–159.
23. Farahbakhsh NA, Cilluffo MC. Synergistic increase in Ca^{2+} produced by A_1 adenosine and muscarinic receptor activation via a pertussis-toxin-sensitive pathway in epithelial cells of the rabbit ciliary body. *Exp Eye Res*. 1997;64:173–179.
24. Farahbakhsh NA, Cilluffo MC. P2 purinergic receptor-coupled signaling in the rabbit ciliary body epithelium. *Invest Ophthalmol Vis Sci*. 2002;43:2317–2325.
25. Ralevic V, Burnstock G. Receptors for purines and pyrimidines. *Pharmacol Rev*. 1998;50:413–492.
26. Kelly SJ, Dardinger DE, Butler LG. Hydrolysis of phosphonate esters catalyzed by 5′-nucleotide phosphodiesterase. *Biochemistry*. 1975;14:4983–4988.
27. Rosenberg PA, Li Y. Forskolin evokes extracellular adenosine accumulation in rat cortical cultures. *Neurosci Lett*. 1996;211:49–52.
28. Rosenberg PA, Li Y. Vasoactive intestinal peptide regulates extracellular adenosine levels in rat cortical cultures. *Neurosci Lett*. 1995;200:93–96.
29. Ziganshin AU, Ziganshina LE, King BE, Burnstock G. Characteristics of ecto-ATPase of Xenopus oocytes and the inhibitory actions of suramin on ATP breakdown. *Pflugers Arch*. 1995;429:412–418.
30. Christoforidis S, Papamarcaki T, Galaris D, Kellner R, Tsolas O. Purification and properties of human placental ATP diphosphohydrolase. *Eur J Biochem*. 1995;234:66–74.
31. Grobben B, Anciaux K, Roymans D, et al. An ecto-nucleotide pyrophosphatase is one of the main enzymes involved in the extracellular metabolism of ATP in rat C6 glioma. *J Neurochem*. 1999;72:826–834.
32. Ohkubo S, Kimura J, Matsuoka I. Correlation between adenine nucleotide-induced cyclic AMP elevation and extracellular adenosine formation in NG108–15 cells. *Jpn J Pharmacol*. 2000;84:325–333.
33. Ohkubo S, Kumazawa K, Sagawa K, Kimura J, Matsuoka I. β,γ-Methylene ATP-induced cAMP formation in C6Bu-1 cells: involvement of local metabolism and subsequent stimulation of adenosine A2B receptor. *J Neurochem*. 2001;76:872–880.
34. Zimmermann H. 5′-Nucleotidase: molecular structure and functional aspects. *Biochem J*. 1992;285:345–365.
35. Ohkubo S, Kimura J, Matsuoka I. Ecto-alkaline phosphatase in NG108–15 cells: a key enzyme mediating P1 antagonist-sensitive ATP response. *Br J Pharmacol*. 2000;131:1667–1672.

36. Zimmermann H. Extracellular metabolism of ATP and other nucleotides. *Naunyn Schmiedebergs Arch Pharmacol*. 2000;362:299–309.
37. Grobben B, Claes P, Roymans D, Esmans EL, Van Onckelen H, Slegers H. Ecto-nucleotide pyrophosphatase modulates the purinoceptor-mediated signal transduction and is inhibited by purinoceptor antagonists. *Br J Pharmacol*. 2000;130:139–145.
38. Khakh BS, Michel AD, Humphrey PP. Inhibition of ectoATPase and Ca-ATPase in rat vas deferens by P2 receptor antagonists (Abstract). *Br J Pharmacol.* 1995;115:2P.
39. Ziganshin AU, Ziganshina LE, King BF, Pintor J Burnstock G. Effects of P2-purinoceptor antagonists on degradation of adenine nucleotides by ecto-nucleotidases in folliculated oocytes of Xenopus laevis. *Biochem Pharmacol*. 1996;51:897–901.
40. Heine P, Braun N, Heilbronn A, Zimmermann H. Functional characterization of rat ecto-ATPase and ecto-ATP diphosphohydrolase after heterologous expression in CHO cells. *Eur J Biochem*. 1999; 262:102–107.
41. Crack BE, Pollard CE, Beukers MW, et al. Pharmacological and biochemical analysis of FPL 67156, a novel, selective inhibitor of ecto-ATPase. *Br J Pharmacol*. 1995;114:475–481.
42. Bruns RF, Fergus JH, Badger EW, et al. Binding of the A_1-selective adenosine antagonist 8-cyclopentyl-1,3-dipropylxanthine to rat brain membranes. *Naunyn-Schmiedebergs Arch Pharmacol*. 1987;335:59–63.
43. Lustig KD, Shiau AK, Brake AJ, Julius D. Expression cloning of an ATP receptor from mouse neuroblastoma cells. *Proc Natl Acad Sci USA*. 1993;90:5113–5117.
44. Fagura MS, Jarvis GE, Dougall IG, Leff P. Adventures in the pharmacological analysis of P2 receptors. *J Auton Nerv Syst*. 2000;81: 166–186.
45. Cilluffo MC, Esqueda E, Farahbakhsh NA. Multiple receptor activation elicits synergistic IP formation in nonpigmented ciliary body epithelial cells. *Am J Physiol Cell Physiol*. 2000;279:C734–C743.
46. Farahbakhsh NA. Purinergic signaling in the rabbit ciliary body epithelium. *J Exp Zool.* In press.
47. Harahap AR, Goding JW. Distribution of the murine plasma cell antigen PC-1 in non-lymphoid tissues. *J Immunol*. 1988;141:2317–2320.
48. Rebbe NF, Tong BD, Finley EM, Hickman S. Identification of nucleotide pyrophosphatase/alkaline phosphodiesterase I activity associated with the mouse plasma cell differentiation antigen PC-1. *Proc Natl Acad Sci USA*. 1991;88:5192–5196.
49. Rebbe NF, Tong BD, Hickman S. Expression of nucleotide pyrophosphatase and alkaline phosphodiesterase I activities of PC-1, the murine plasma cell antigen. *Mol Immunol*. 1993;30:87–93.
50. van Driel IR, Wilks AF, Pietersz GA, Goding JW. Murine plasma cell membrane antigen PC-1: molecular cloning of cDNA and analysis of expression. *Proc Natl Acad Sci USA*. 1985;82:8619–8623.
51. Stracke ML, Krutzsch HC, Unsworth EJ, et al. Identification, purification, and partial sequence analysis of autotaxin, a novel motility-stimulating protein. *J Biol Chem*. 1992;267:2524–2529.
52. Narita M, Goji J, Nakamura H, Sano K. Molecular cloning, expression, and localization of a brain-specific phosphodiesterase I/nucleotide pyrophosphatase (PD-Iα) from rat brain. *J Biol Chem*. 1994;269:28235–28242.
53. Deissler H, Lottspeich F, Rajewsky MF. Affinity purification and cDNA cloning of rat neural differentiation and tumor cell surface antigen gp130^{RB13-6} reveals relationship to human and murine PC-1. *J Biol Chem*. 1995;270:9849–9855.
54. Jin-Hua P, Goding JW, Nakamura H, Sano K. Molecular cloning and chromosomal localization of PD-Iβ (PDNP3), a new member of the human phosphodiesterase I genes. *Genomics*. 1997;45:412–415.
55. Lambrecht G, Friebe T, Grimm U, et al. PPADS, a novel functionally selective antagonist of P2 purinoceptor-mediated responses. *Eur J Pharmacol*. 1992;217:217–219.
56. Kennedy C, Westfall TD, Sneddon P. Modulation of purinergic neurotransmission by ecto-ATPase. *Semin Neurosci*. 1996;8:195–199.
57. Charlton SJ, Brown CA, Weisman GA, Turner JT, Erb L, Boarder MR. PPADS and suramin as antagonists at cloned P2Y- and P2U-purinoceptors. *Br J Pharmacol*. 1996;118:704–710.
58. Westfall TD, Kennedy C, Sneddon P. The ecto-ATPase inhibitor ARL 67156 enhances parasympathetic neurotransmission in the guinea-pig urinary bladder. *Eur J Pharmacol*. 1997;329:169–173.
59. Dowd FJ, Li LS, Zeng W. Inhibition of rat parotid ecto-ATPase activity. *Arch Oral Biol*. 1999;44:1055–1062.
60. Westfall TD, Menzies JR, Liberman R, et al. Release of a soluble ATPase from the rabbit isolated vas deferens during nerve stimulation. *Br J Pharmacol*. 2000;131:909–914.
61. Westfall TD, Sarkar S, Ramphir N, Westfall DP, Sneddon P, Kennedy C. Characterization of the ATPase released during sympathetic nerve stimulation of the guinea-pig isolated vas deferens. *Br J Pharmacol*. 2000;129:1684–1688.
62. Burger RM, Lowenstein JM. 5′-Nucleotidase from smooth muscle of small intestine and from brain: inhibition of nucleotides. *Biochemistry*. 1975;14:2362–2366.
63. Bankir L, Ahloulay M, Devreotes PN, Parent CA. Extracellular cAMP inhibits proximal reabsorption: are plasma membrane cAMP receptors involved? *Am J Physiol*. 2002;282:F376–F392.
64. Stefanovic V, Mandel P, Rosenberg A. Ecto-5′-nucleotidase of intact cultured C6 rat glioma cells. *J Biol Chem*. 1976;251:3900–3905.
65. von Kugelgen I, Wetter A. Molecular pharmacology of P2Y-receptors. *Naunyn Schmiedebergs Arch Pharmacol*. 2000;362:310–323.
66. Sears ML. The aqueous. In: Moses RA, ed. *Adler's Physiology of the Eye: Clinical Application.* St. Louis, MO: CV Mosby Company; 1981;204–226.